Tracking-FCS: Fluorescence correlation spectroscopy of individual particles

Andrew J. Berglund and Hideo Mabuchi

Physical Measurement and Control 266-33
California Institute of Technology, Pasadena, CA 91125

berglund@caltech.edu

Abstract: We exploit recent advances in single-particle tracking to perform fluorescence correlation spectroscopy on *individual* fluorescent particles, in contrast to traditional methods that build up statistics over a sequence of many measurements. By rapidly scanning the focus of an excitation laser in a circular pattern, demodulating the measured fluorescence, and feeding these results back to a piezoelectric translation stage, we track the Brownian motion of fluorescent polymer microspheres in aqueous solution in the plane transverse to the laser axis. We discuss the estimation of particle diffusion statistics from closed-loop position measurements, and we present a generalized theory of fluorescence correlation spectroscopy for the case that the motion of a single fluorescent particle is actively tracked by a time-dependent laser intensity. We model the motion of a tracked particle using Ornstein-Uhlenbeck statistics, using a general theory that contains a number of existing results as specific cases. We find good agreement between our theory and experimental results, and discuss possible future applications of these techniques to passive, single-shot, single-molecule fluorescence measurements with many orders of magnitude in time resolution.

OCIS codes: (180.2520) Fluorescence microscopy; (180.5810) Scanning microscopy; (300.6280) Spectroscopy, fluorescence and luminescence

References and links

1. D. Magde, E. L. Elson, and W. W. Webb, "Thermodynamic fluctuations in a reacting system - measurement by fluorescence correlation spectroscopy," Phys. Rev. Lett. **29,** 705-708 (1972).
2. E. L. Elson and D. Magde, "Fluorescence correlation spectroscopy. 1. Conceptual basis and theory," Biopolymers **13,** 1-27 (1974).
3. D. Magde, E. L. Elson, and W. W. Webb, "Fluorescence correlation spectroscopy. 2. Experimental realization," Biopolymers **13,** 29-61 (1974).
4. O. Krichevsky and G. Bonnett, "Fluorescence correlation spectroscopy: the technique and its applications," Rep. Prog. Phys. **65,** 251-297 (2002).
5. S. T. Hess, S. Huang, A. A. Heikal, and W. W. Webb, "Biological and Chemical Applications of Fluorescence Correlation Spectroscopy: A Review," Biochemistry **41,** 697-705 (2002).
6. A. J. Berglund, A. C. Doherty, and H. Mabuchi, "Photon statistics and dynamics of Fluorescence Resonance Energy Transfer," Phys. Rev. Lett. **89,** 068101 (2002).
7. H. D. Kim, G. U. Nienhaus, T. Ha, J. W. Orr, J. R. Williamson, and S. Chu, "Mg^{2+}-dependent conformational changes of RNA studied by fluorescence correlation and FRET on immobilized single molecules," Proc. Natl. Acad. Sci. U.S.A. **99,** 4284-4289 (2002).
8. K. C. Neuman and S. M. Block, "Optical Trapping," Rev. Sci. Instrum. **75,** 2787-2809 (2004).
9. M. J. Saxton and K. Jacobson, "Single-particle tracking: applications to membrane dynamics," Annu. Rev. Biophys. Biomolec. Struct. **26,** 373-399 (1997).
10. A. E. Cohen and W. E. Moerner, "Method for trapping and manipulating nanoscale objects in solution," Appl. Phys. Lett. **86,** 093109 (2005).

#8420 - $15.00 USD Received 9 August 2005; revised 20 September 2005; accepted 21 September 2005

11. A. E. Cohen, "Control of Nanoparticles with Arbitrary Two-Dimensional Force Fields," Phys. Rev. Lett. **94,** 118102 (2005).
12. T. Meyer and H. Schindler, "Simultaneous Measurement of Aggregation and Diffusion of Molecules in Solutions and in Membranes," Biophys. J. **54,** 983-993 (1988).
13. T. Ha, D. S. Chemla, T. Enderle, and S. Weiss, "Single molecule spectroscopy with automated positioning," Appl. Phys. Lett. **70,** 782-784 (1997).
14. J. Enderlein, "Tracking of fluorescent molecules diffusing within membranes," Appl. Phys. B **71,** 773-777 (2000).
15. J. Enderlein, "Positional and Temporal Accuracy of Single Molecule Tracking," Sing. Mol. **1,** 225-230 (2000).
16. R. S. Decca, C.-W. Lee, and S. R. Wassall, "Single molecule tracking scheme using a near-field scanning optical microscope," Rev. Sci. Instr. **73,** 2675-2679 (2002).
17. V. Levi, Q. Ruan, K. Kis-Petikova, and E. Gratton, "Scanning FCS, an novel method for three-dimensional particle tracking," Biochem. Soc. Trans. **31,** 997-1000 (2003).
18. A. J. Berglund and H. Mabuchi, "Feedback controller design for tracking a single fluorescent molecule," Appl. Phys. B **78,** 653-659 (2004).
19. K. Kis-Petikova and E. Gratton, "Distance measurement by circular scanning of the excitation beam in a two-photon microscope," Microsc. Res. Tech. **63,** 34-49 (2004).
20. V. Levi, Q. Ruan, and E. Gratton, "3-D particle tracking in a two-photon microscope. Application to the study of molecular dynamics in cells," Biophys. J. **88,** 2919-2928 (2005).
21. M. A. Digman, P. Sengupta, P. W. Wiseman, C. M. Brown, A. R. Horwitz, and E. Gratton, "Fluctuation Correlation Spectroscopy with a Laser-Scanning Microscope: Exploiting the Hidden Time Structure," Biophys. J. **88,** L33-L36 (2005).
22. M. A. Digman, C. M. Brown, P. Sengupta, P. W. Wiseman, A. R. Horwitz, and E. Gratton, "Measuring fast dynamics in solutions and cells with a laser scanning microscope," Biophys. J. **89,** 1317-1327 (2005).
23. M. H. DeGroot, *Probability and Statistics* (Addison-Wesley, Reading, MA, 1986).
24. G. Chirico, C. Fumagalli, and G. Baldini, "Trapped Brownian Motion in Single- and Two-Photon Excitation Fluorescence Correlation Experiments," J. Phys. Chem. B **106,** 2508-2519 (2002).
25. C. W. Gardiner, *Handook of Stochastic Methods for Physics, Chemistry and the Natural Sciences*, 2nd ed. (Springer-Verlag, 1985).
26. N. G. Van Kampen, *Stochastic processes in physics and chemistry* (Elsevier Science Pub. Co., North-Holland, Amsterdam, 2001).
27. A. Gennerich and D. Schild, "Fluorescence correlation spectroscopy in small cytosolic compartments depends critically on the diffusion model used," Biophys. J. **79,** 3294-3306 (2000).
28. A. J. Berglund and H. Mabuchi, "Performance bounds on single-particle tracking by fluorescence modulation," in preparation (2005).
29. X. Zhuang, L. E. Bartley, H. P. Babcock, R. Russell, T. Ha, D. Hershlag, and S. Chu, "A Single-Molecule Study of RNA Catalysis and Folding," Science **288,** 2048-2051 (2000).
30. B. Okumus, T. J. Wilson, D. M. J. Lilley, and T. Ha, "Vesicle Encapsulation Studies Reveal that Single Molecule Ribozyme Heterogeneities Are Intrinsinc," Biophys. J. **87,** 2798-2806 (2004).
31. E. Rhoades, E. Gussakovsky, and G. Haran, "Watching proteins fold one molecule at a time," Proc. Natl. Acad. Sci. U.S.A. **100,** 3197-3202 (2003).

1. Introduction

Since its inception more than 30 years ago, fluorescence correlation spectroscopy (FCS) has provided an experimental technique for investigating molecular motions and kinetics at the scale of only a few molecules [1, 2, 3]. A significant advantage of FCS is that it provides simple data analysis procedures for exploiting the high time-resolution of single-photon counting methods. FCS can be used to measure diffusion, conformational fluctuations and chemical kinetics over many timescales with little modification to the original technique [4, 5]. However, FCS requires both a small excitation volume and a low concentration of analyte particles. These requirements lead to the major disadvantages of the technique: long data acquisition times are imposed by the low analyte concentration, since the time a typical particle of interest spends in the laser focus is necessarily on the order of the time between transits, and the localized excitation intensity precludes widefield spatial sensitivity. Because of the small observation time per particle, the resolution of fast timescale dynamics requires averaging over an ensemble of many individual molecular transits, perhaps hundreds or thousands [6]. Partly in response to this problem, sophisticated experimental methods have been developed for detecting larger-scale spatial information and increasing the data acquisition time per particle by surface-immobilization [7],

#8420 - $15.00 USD Received 9 August 2005; revised 20 September 2005; accepted 21 September 2005

optical trapping [8], single-particle tracking by video microscopy [9], and trapping via recently developed electrophoretic methods [10, 11]. However, all of these techniques require the application of local forces, or involve a sacrifice in time resolution arising from charge-coupled device imaging methods.

More recently, new experimental and theoretical techniques have been developed that may improve this compromise between mesoscale spatial information, time-resolution, environmental modification, and the rate of data acquisition in single-molecule spectroscopy. In particular, many groups have employed a time-varying laser intensity (either rotating or scanning) for extracting position information from fluorescent particles. As usual, it is necesary to use noise correlation techniques to extract information from noisy, stochastic data. A prominent early example of the utility of a time-varying laser intensity for extracting position information from diffusing particles was given by Meyer [12]. In that work, a rotating laser was used to measure diffusion coefficients and aggregation. Since then, methods of feedback tracking using a time-varying laser intensity to estimate a particle's position have been developed in various proposals and experiments [13, 14, 15, 16, 17, 18, 19, 20]. In addition to temporal autocorrelation techniques, video imaging and spatial autocorrelation techniques may be combined with laser-scanning methods in order to improve temporal and spatial resolution in measuring diffusive particle dynamics [21, 22]. A common requirement among all of these techniques is a simple theory for interpreting experimental correlation function measurements.

In this paper, we return to recent results on feedback-tracking of single diffusing particles in an epifluorescence confocal microscope. Three-dimensional tracking of fluorescent microspheres in a Gaussian laser has been demonstrated by the group of Gratton *et. al.* [17, 19, 20]. They operate in a regime where particle motion is substantially slower than the feedback control bandwidth, so that fluorescence fluctuations are essentially negligible and the tracking controller's position provides a high-resolution estimate of the tracked particle's position. Of course, one cannot track a particle whose motion is faster than the available feedback bandwidth; however, it is possible to track diffusing particles whose motion is comparable to the feedback bandwidth. We are interested in extending the bandwidth limits of the tracking performance and studying the information that can be acquired in this regime where a particle's motion is comparable to the response speed of the feedback controller. Our eventual goal is to track individual biological molecules in free solution, while maintaining high time-resolution fluorescence detection capability; since biological molecules may move with much larger diffusion coefficients than the fluorescent beads studied to date, we will certainly require both experimental and theoretical methods for particle tracking and fluorescence correlation measurements on fast moving particles. It is the goal of this paper to develop these latter methods. In this case, fluorescence fluctuations arise from particle motion as well as feedback controller dynamics. In the present work, we show that fluorescence fluctuations from a tracked particle contain useful information that can be exploited by theoretical methods in a manner analogous to the theory of FCS, even at timescales comparable to the response bandwidth of the tracking control. The tracking feedback signal contains information about the particle's diffusion statistics along the tracked degrees of freedom, while the residual fluorescence fluctuations contain information about uncontrolled particle motion and feedback controller dynamics. This "tracking-FCS" is non-invasive, in that it does not require trapping forces, and it permits high-time resolution fluorescence detection over long observation periods on individual particles, thus reducing the reliance on ensemble averages to resolve fast fluctuations. Tracking-FCS methods preserve the time-resolution and single-particle sensitivity of traditional FCS in solution while affording many advantages previously reserved for immobilization and trapping methods.

#8420 - $15.00 USD Received 9 August 2005; revised 20 September 2005; accepted 21 September 2005

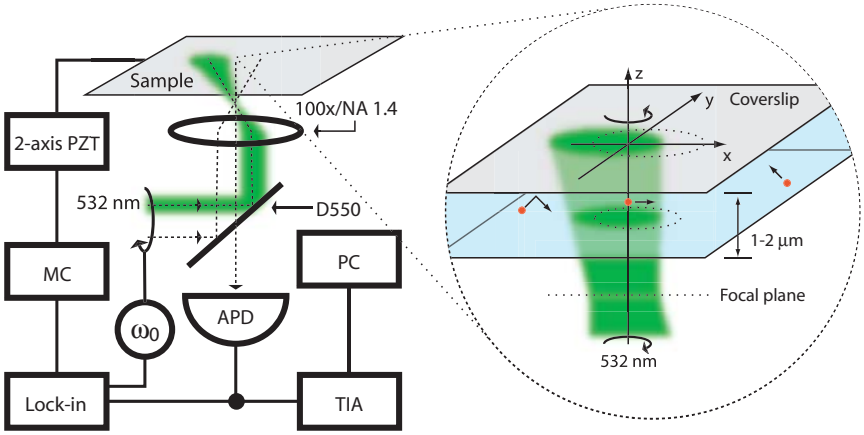

Fig. 1. (Left) Schematic diagram of the optics and electronics for tracking-FCS. Key: TIA = time-interval analyzer, APD = avalanche photodiode, MC = microcontroller, PZT = piezoelectric translation stage, D550 = dichroic filter with 550 nm cutoff. (Right) Detail of the sample volume. 60-nm diameter fluorescent beads suspended in water diffuse freely in the *xy* plane, but are confined by glass coverslips in the *z* direction. The coverslips are mounted on a piezoelectric sample stage, so that the entire bulk fluid volume can be translated. A tracked particle diffuses freely (in the axially confined geometry) in the reference frame of the bulk fluid while the feedback control translates the entire sample volume in order to hold the particle on the laser axis defined by $x = y = 0$. Because the sense of the laser rotation, and therefore the sign of the feedback controller, reverses upon crossing the focal plane of the microscope optics, the sample mount is adjusted in the *z* direction so that the focal plane lies just outside of the sample volume.

2. Experimental methods and results

In order to collect high time-resolution fluorescence information from free particles in solution, we use a home-built single-particle tracking confocal microscope, operating in epifluorescence configuration using a 100x/NA 1.4 oil-immersion microscope objective (Carl Zeiss, Inc., Thornwood, NY). Diagrams of the tracking apparatus and sample volume are shown in Fig. 1. Fluorescence light is collected from free particles in solution as they diffuse into and out of the diffraction-limited laser focus. Fluorescence light is collected by the same microscope objective, separated from the excitation light using dichroic filters, and imaged onto single-photon counting avalanche photodiodes (PerkinElmer, Wellesley, MA). The photon arrival time signal is electronically split into two copies, with one branch recorded using a time-interval analyzer (Guide Technologies, Sunnyvale, CA) and the other branch sent to a lock-in amplifier for tracking control. The time-interval analyzer records the arrival time of each photon with 0.5 ns accuracy. This photon arrival time information is saved to a desktop computer, and fluorescence time traces and autocorrelation functions are obtained by post-analysis of the recorded data.

The basic idea behind our tracking microscope is the implementation of a feedback controller for translating the entire sample stage in the *xy*-plane perpendicular to the excitation laser axis, such that the particle diffuses freely within the sample volume but nonetheless remains within the laser focus. Our experimental method differs from that of Gratton *et. al.* primarily in the signal processing and controller methods described in this section. In our experiment, particle tracking occurs in two steps. First, a particle moves away from the axis of laser rotation by free diffusion. This off-axis position is detected by the fluorescence modulation/demodulation

#8420 - $15.00 USD Received 9 August 2005; revised 20 September 2005; accepted 21 September 2005

scheme described below. Second, the off-axis position of the particle is electronically fed back to a piezoelectric sample mount, which translates the entire sample stage to move the particle back onto the axis of laser rotation. The entire closed-loop apparatus then serves to "hold" the particle on the axis of laser rotation by translating the bulk sample stage to compensate for the particle's diffusive motion. It should be emphasized that the entire feedback control process is performed using only the photon arrival time signal, with no video imaging or in-loop computer processing. In this way, we maintain the high time-resolution associated with time-correlated single-photon counting fluorescence methods, while the lock-in technique utilized here enables extension of the tracking approach to particles with much larger diffusion coefficients (approaching those of biomolecules in water [18]). See Fig. 1 for a block diagram of the detection and signal processing optics and electronics.

In order to estimate the particle's off-axis position, we use resonant beam deflectors operating at $\omega_0 = 2\pi \times 8$ kHz in order to translate the excitation laser in a circular path about its axis. This circular motion modulates the laser intensity at off-axis positions within the sample volume (on-axis, a particle sees constant laser intensity). We estimate a particle's position by demodulating the fluorescence signal at the laser rotation frequency using a lock-in amplifier. The resulting *xy* position estimates are filtered by a programmable microcontroller (Analog Devices, Norwood, MA; Keil μVision software, Plano, TX) and fed back to a two-axis piezoelectric sample stage (Polytec PI, Inc., Auburn, MA) that translates the entire sample volume. A stochastic state-space model of this system along with optimal feedback controller design methods that incorporate realistic experimental limitations, such as noisy fluorescence measurements and piezo-actuator bandwidths, can be found in [18]. In the present experimental realization, we use a simplified proportional-integral feedback controller though we hope to improve the tracking bandwidth using the controllers designed in [18].

To see why lock-in detection provides a suitable feedback error signal, consider a Gaussian laser with beam waist w_{xy} rotating at a radius r_0 and angular frequency ω_0 about its direction of propagation. In any fixed plane perpendicular to the axis of rotation, we may approximate the rate of photon detection from a particle at position $(x,y) \mapsto (\rho,\theta)$ by a two dimensional Gaussian "detectivity" function, given in cylindrical coordinates by

$$\Phi_t(\rho,\theta) \quad = \quad \exp\left\{ -\frac{2}{w_{xy}^2}\left[(\rho\cos\theta - r_0\cos\omega_0 t)^2 + (\rho\sin\theta - r_0\sin\omega_0 t)^2 \right] \right\}. \qquad (1)$$

Throughout the paper, we will use units such that the peak photon detection rate is unity. For lock-in detection of the fluorescence at the rotation frequency ω_0, the quadrature outputs are given by the cosine and sine transforms of $\Phi_t(\rho,\theta)$ at frequency ω_0. Denoting these quadratures by $f_c(\rho,\theta)$ and $f_s(\rho,\theta)$ respectively, we find (neglecting finite-bandwidth filtering at the lock-in amplifier's output)

$$f_c(\rho,\theta) = h(\rho)\cos\theta \quad , \quad f_s(\rho,\theta) = h(\rho)\sin\theta \qquad (2)$$

where

$$h(\rho) = 2\pi\frac{\Gamma_0}{\omega_0}\exp\left[-\frac{2}{w_{xy}^2}\left(\rho^2 + r_0^2\right)\right] I_1\left[\frac{4r_0\rho}{w_{xy}^2}\right]. \qquad (3)$$

I_1 is the modified Bessel function of order 1. This pair of transformations maps curves in the (x,y) plane to curves in the (f_c, f_s) plane, with the convenient property that the angular coordinate θ is unchanged. Lock-in detection may therefore incorrectly estimate the *distance* of a particle from the origin, but never the *direction*. In the limit $\rho/w_{xy} \ll 1$, with $r_0 \sim w_{xy}$, we have

$$h(\rho) \approx 4\pi\frac{r_0\rho}{w_{xy}^2}\exp\left[-2\frac{r_0^2}{w_{xy}^2}\right]. \qquad (4)$$

#8420 - $15.00 USD Received 9 August 2005; revised 20 September 2005; accepted 21 September 2005

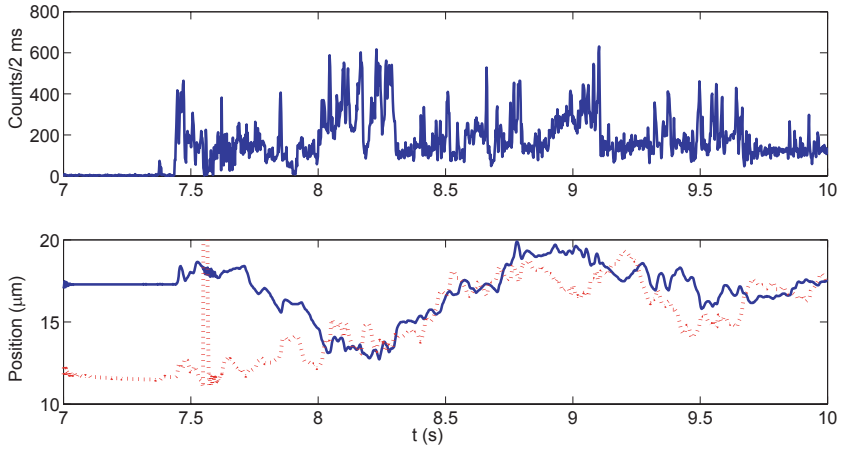

Fig. 2. Fluorescence data and motion of the sample stage during tracking of a 60 nm microsphere in water. The upper plot shows fluorescence data, and the lower plot shows the *x* (solid) and *y* (dotted) positions of the sample stage during the fluorescence trace. Just before 7.5 s, a particle diffused into the capture region and the controller correspondingly responded by moving the sample stage to track this particle. The irregular motion of the sample stage at 7.6 s resulted from an (expected) arithmetic overflow in the microcontroller. The residual fluorescence fluctuations during tracking arise from the competition between diffusion and feedback control and also from the uncontrolled motion of the particle in the *z* direction. The fluctuations are recorded in Fig. 4 and a detailed theory is given in the next section.

The above fact, that $h(\rho) \propto \rho$ for small ρ, shows that the lock-in output is a *linear* function of the particle's position near the origin and provides an error signal suitable for feedback control. While a particle is locked to the laser axis by the feedback controller, the non-linear character of $h(\rho)$ is not apparent. This is a general strategy for feedback control in mildly non-linear systems, in which a suitable control law linearizes the system dynamics about a fixed point. Note that when a rotating laser is focused through a microscope objective, the beam converges and then diverges, with the proportionality constant between the particle position and the linearized lock-in quadrature outputs becoming a function of the axial coordinate *z*, changing signs upon passing through the focal plane (See Fig. 1). In this way, we see that our two-dimensional controller may track transverse motion over a range of depths, so long as the control law provides enough gain margin to absorb the variation in position estimation and provided that the sample volume does not cross the focal plane.

For the measurements described in this paper, 60-nm diameter polystyrene microspheres embedded with "Envy green" fluorophores were purchased from a commercial vendor (Bangs Laboratories, Inc., Fishers, IN); each bead contains many fluorophores. Microspheres were suspended in de-ionized water. No. 1 glass microslide coverslips were immersed in 1M KOH for 30 minutes to minimize surface impurities. In a typical experiment, 2 μl, 0.1 nM solution of microspheres was placed between glass cover slips. We used excitation light with 532 nm wavelength and only $\sim 1-10\mu$W optical power for exciting the fluorescently-labelled beads. Our overall photon count rates of $\sim 10^5$/s are comparable to the count rates from individual dye molecules excited by a correspondingly higher laser power. In this configuration, the fluorescent beads provide a good test-case toward the eventual goal of tracking individual molecules

#8420 - $15.00 USD Received 9 August 2005; revised 20 September 2005; accepted 21 September 2005

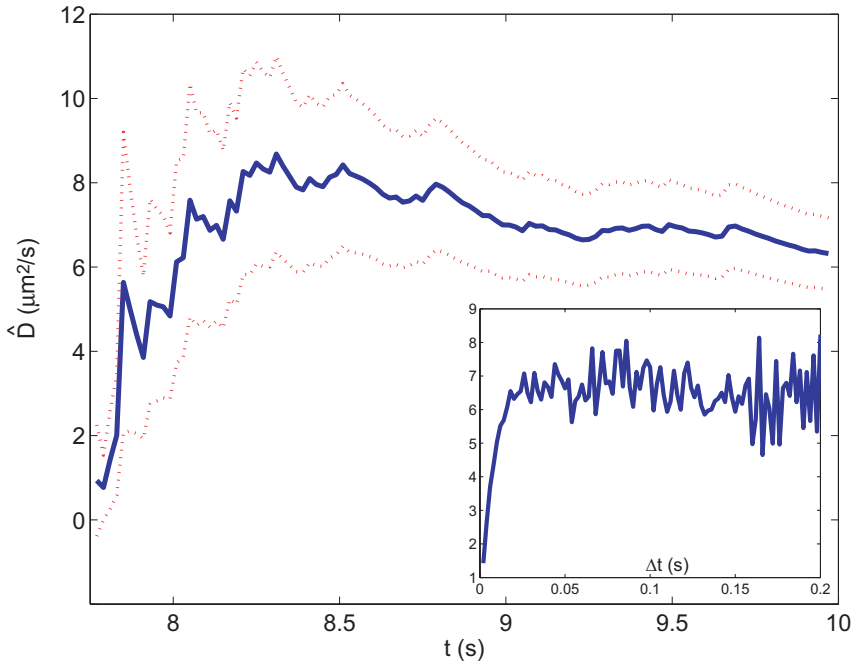

Fig. 3. Time-converging estimate of the diffusion coefficient D for the microsphere tracking data in Fig. 2 with bin time $\Delta t = 20$ ms. The dotted lines are error estimates calculated for the estimator $\hat{D}$, assuming underlying Brownian statistics. Inset: Final estimate of D as a function of bin time Δt. For bin times larger than ~ 10 ms, the estimates are roughly constant with mean value $D = 6.2\ \mu\text{m}^2/\text{s}$. See the text for an explanation of the estimator convergence with Δt.

labelled with a single fluorescent marker. The z position of the objective was adjusted such that the focus lay just outside the sample boundary, so that the particle cannot diffuse across the focal plane of the microscope objective. In calibration experiments at high fluorophore concentration, we have estimated the depth of our sample in this configuration to be $\sim 1\mu$m (see Fig. 1).

An example of the tracking microscope's performance is shown in Fig. 2. From the data in the figure, we see that the tracking controller maintains a relatively constant fluorescence intensity for about 2.5 s, while the stage position moves well over 10 μm along both the x and y axes. The residual fluctuations in the fluorescence will be discussed in detail in the next section. Here, we simply remark that they arise from the feedback control bandwidth and also from the uncontrolled motion of the particle in the axial (z) direction.

We may estimate the isotropic diffusion coefficient D for this microsphere from the position of the sample stage during tracking. While the particle is (approximately) locked on the laser axis by the feedback controller, the xy position of the sample stage provides a bandwidth-limited filtration of the particle's position. Let the change in a particle's x position during a time interval Δt be given by Δx, and similarly for y. Then we may construct a simple estimator $\hat{D}$ for a particle's diffusion coefficient D based on the sample stage trajectory:

$$\hat{D} = \left[\left\langle (\Delta x)^2 \right\rangle + \left\langle (\Delta y)^2 \right\rangle\right] / (4\Delta t) \tag{5}$$

where the angle brackets denote time-averaging over the sample trajectory, sectioned into bins

#8420 - $15.00 USD Received 9 August 2005; revised 20 September 2005; accepted 21 September 2005

of size Δt. If Δt is smaller than the inverse closing bandwidth of the controller, then the sample stage will exhibit reduced variations on this timescale, and we will tend to underestimate the resulting diffusion coefficient with Eq. (5). It is easy to see this by considering an extreme case: imagine binning the particle's position over extremely small intervals, much smaller than the response time of our piezoelectric sample stage (say, 1 μs). Then in each time interval Δt, the sample stage cannot track the diffusing particle (although the particle does not move far enough to escape the tracking controller) and only follows an "average" trajectory. The sample stage will move a distance proportional to Δt (*i.e.* at a fixed velocity along the averaged particle trajectory) for these very small bin times, while the particle itself moves a distance proportional to $\sqrt{\Delta t}$ (the characteristic property of Brownian motion). For small enough Δt, then, the estimator given by Eq. (5) will dramatically underestimate the particle's diffusion coefficient (by a factor proportional to $\sqrt{\Delta t}$). As Δt becomes much larger than the inverse closing bandwidth, however, the sample stage can move sufficiently fast to track the detailed motion of the particle within a single bin interval. In this case, we expect a good statistical estimate of D from Eq. (5), but with a concomitant increase in the estimator variance due to the smaller number of bin intervals per fixed-length trajectory. Estimates constructed in this way are shown in Fig. 3, along with error bars calculated for the estimator Eq. (5) assuming underlying Brownian motion statistics (see [23] for details about statistical estimation and error estimates). For large bin times, the estimate of D converges to a value 6.2 $\mu\text{m}^2/\text{s}$, close to the value 7.2 $\mu\text{m}^2/\text{s}$ predicted by the Stokes-Einstein relation for 60 nm-diameter beads in water at room temperature. It is possible that surface adhesion slightly reduced the effective diffusion coefficient, or that this particular microsphere was closer to 70 nm in diameter, than the batch average of 60 nm. We do not suspect induced optical dipole forces to give any significant trapping effect, since only a moderate trapping effect was observed for 1 mW of near-IR laser power on microspheres with 276 nm diameter in [20], whereas we use smaller microspheres and only 1-10 μW of 532 nm light. A detailed analysis of optical trapping effects in FCS experiments can be found in [24].

3. Fluorescence fluctuations and Tracking-FCS

It is clear from the data in Fig. 2 that there are residual fluctuations in the recorded fluorescence during the tracking period. We attribute these fluctuations to two dynamical effects on two separate timescales. First, in the regime where the particle's diffusive motion is not well-separated from the tracking-controller bandwidth, we expect significant fluctuations from uncontrolled transverse motion of the particle within the excitation laser. This uncontrolled motion is not (on average) fast enough for the particle to escape from the laser focus, but it does contribute to fluorescence fluctuation. Second, we expect significant fluctuation arising from motion along the uncontrolled z direction. In this section, we develop a full theoretical model for the residual fluorescence fluctuations that arise during a typical tracking period under Gaussian illumination. With this model, we may study the both the dynamics of the feedback controller and also the intrinsic statistics of the particle's diffusive motion solely by examining fluorescence fluctuation statistics. In this way, our theory is analogous to the theory of FCS. The main ingredient of our model is the use of Ornstein-Uhlenbeck statistics (see below) for modelling the motion of a tracked (or trapped) particle.

While a particle is being tracked by the rotating laser, the sample stage is actuated to hold the particle at the origin of coordinates. We may therefore consider the particle to be *trapped* in the laboratory reference frame. We will no longer model the particle as a free Brownian particle in the frame of the sample stage; rather, we characterize the action of the tracking controller as a *damping force* centered at the coordinate origin (the lock-point of the tracking controller). Since diffusion along the Cartesian axes is independent, consider the particle's motion along one axis

#8420 - $15.00 USD Received 9 August 2005; revised 20 September 2005; accepted 21 September 2005

only. Let the particle's position be given by X_t and its diffusion coefficient be D. The damping force due to tracking may be modelled as a rate γ_x, the step-response of the closed-loop servo system, such that the particle's position follows an approximate Ornstein-Uhlenbeck process:

$$dX_t = -\gamma_x X_t dt + \sqrt{2D} dW_t \tag{6}$$

where dW_t is the differential of a Wiener process [25, 26]. Equation (6) is a stochastic differential equation whose solutions X_t satisfy Ornstein-Uhlenbeck statistics for the stationary distribution $P_0(x) \equiv \lim_{t\to\infty} P(X_t = x)$ and transition probability $P_\tau(x_2|x_1) \equiv \lim_{t\to\infty} P(X_{t+\tau} = x_2|X_t = x_1)$:

$$P_0(x) = \frac{1}{\sqrt{2\pi\vec{x}^2}} \exp\left[-\frac{x^2}{2\vec{x}^2}\right] \tag{7}$$

$$P_\tau(x_2|x_1) = \frac{1}{\sqrt{2\pi b_\tau^2}} \exp\left[-\frac{(x_2 - a_\tau x_1)^2}{2b_\tau^2}\right] \tag{8}$$

where $a_\tau = \exp(-\gamma_x\tau)$, $b_\tau^2 = \vec{x}^2\left[1 - \exp(-2\gamma_x\tau)\right]$ and the length-scale is given $\vec{x}^2 = D/\gamma_x$. We consider only stationary distributions, since we are interested in the steady-state of the tracking controller, not initial transients.

We may now calculate the fluorescence autocorrelation function for a single diffusing particle trapped at the coordinate origin and illuminated by a Gaussian laser whose centroid follows an *arbitrary* time-dependent path $x_t^{(L)} = w_x\chi_t$ (in one dimension only), where χ_t is the dimensionless laser path written in units of the beam waist w_x. We assume the laser intensity $\Phi_x(x)$ is Gaussian with beam waist w_x, so that the rate of photon detections is also Gaussian with the same waist. The fluorescence autocorrelation function is given in this case by

$$G(\tau) = \left\langle \iint dx_1 dx_2 P_\tau(x_2|x_1) P_0(x_1) \Phi_x(x_2 - w_x\chi_{t+\tau}) \Phi_x(x_1 - w_x\chi_t) \right\rangle_t \tag{9}$$

where the angle brackets denote an average over t. See Appendix A for a derivation of Eq. (9). It is convenient to define a dimensionless "confinement parameter" ζ_x by

$$\zeta_x = \frac{\gamma_x\tau_x}{1 + \gamma_x\tau_x} = \frac{w_x^2}{w_x^2 + 4\vec{x}^2} \tag{10}$$

where $\tau_x = w_x^2/4D$ is the usual diffusion time. ζ_x is a measure of the localization of the trapped particle with respect to the excitation beam waist. Free Brownian motion results are recovered in the limit $\gamma_x \to 0$ ($\zeta_x \to 0$), while $\gamma_x \to \infty$ ($\zeta_x \to 1$) represents the perfect tracking limit.

Consider the right-hand side of Eq. (9) without the angle brackets. Denoting this term by $\mathscr{G}_x(\tau;\chi_t)$, we may explicitly evaluate for Gaussian Φ_x and probabilities given by Eqs. (7) and (8):

$$\mathscr{G}_x(\tau;\chi_t) = \frac{\zeta_x}{\sqrt{1 - \lambda_{\tau,x}^2}} \exp\left[-2\zeta_x\left(\frac{\chi_{t+\tau}^2 - 2\lambda_{\tau,x}\chi_t\chi_{t+\tau} + \chi_t^2}{1 - \lambda_{\tau,x}^2}\right)\right] \tag{11}$$

where

$$\lambda_{\tau,x} = (1 - \zeta_x)\, e^{-\gamma_x\tau}. \tag{12}$$

Equation (11) specifies the one-dimensional fluorescence autocorrelation through the time average $G(\tau) = \langle \mathscr{G}_x(\tau;\chi_t)\rangle_t$. If we now consider a full three-dimensional case, in which the

#8420 - $15.00 USD Received 9 August 2005; revised 20 September 2005; accepted 21 September 2005

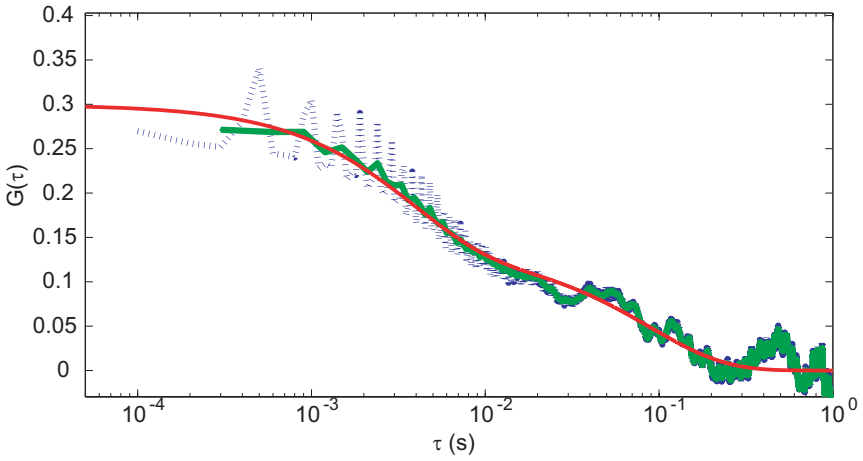

Fig. 4. Fluorescence correlation functions recorded during the tracking period in Fig. 2, normalized to the mean fluorescence. The noisy curves were measured from the tracking data in Fig. 2, averaged over coarse-grained time bins of 100 (dotted) and 200 (solid) μs. At higher time resolution, the oscillations due to the deterministic laser rotation make it difficult to resolve the overall shapes of the autocorrelation curve. The smooth solid curve is a fit to Eq. (18). The fit parameters are $\gamma_{xy} = 134$ Hz, $D = (6.2\ \mathrm{s}^{-1})w_{xy}^2$, $\rho_0 = 1.4w_{xy}$, $\gamma_z = 11.3$ Hz, $w_z = 4.5\mu$m, and $z_0 = 2.8w_{xy}$. γ_{xy} is the tracking controller bandwidth. All fit parameters are scaled by the true beam waist w_{xy}, which is approximately 1μm. For this value, the diffusion coefficient D determined by the statistical estimate from Fig. 3 and the value from a fit to Eq. 18 are identical.

particle is trapped with rate γ_k along axis $k \in \{x,y,z\}$ in a Gaussian laser with waist w_k in the k direction, and the laser centroid follows the three-dimensional path $\mathbf{r}_t$, we have an explicit expression for the full fluorescence autocorrelation function

$$G(\tau) = \left\langle \mathscr{G}_x\left(\tau; \frac{\hat{\mathbf{x}}\cdot\mathbf{r}_t}{w_x}\right) \mathscr{G}_y\left(\tau; \frac{\hat{\mathbf{y}}\cdot\mathbf{r}_t}{w_y}\right) \mathscr{G}_z\left(\tau; \frac{\hat{\mathbf{z}}\cdot\mathbf{r}_t}{w_z}\right) \right\rangle_t \tag{13}$$

where the hat ˆ denotes Cartesian unit vectors. Equation (13) is a general result for a fluorescent particle undergoing three-dimensional, asymmetric Ornstein-Uhlenbeck diffusion in a three-dimensional Gaussian laser whose centroid follows the path $\mathbf{r}_t$. It reproduces the usual results for free Brownian motion ($\gamma_k = 0$) and time-independent laser intensity ($\mathbf{r}_t = \mathbf{r}_0$) in the appropriate limits.

A number of models in the literature are contained in the general form of 13. For $\mathbf{r}_t$ constant and $\gamma_k = 0$, Eq. (13) reproduces the standard FCS result. For $\gamma_k = 0$ and $\mathbf{r}_t$ describing a two-dimensional circular orbit with the radius of rotation much larger than the beam waist, Eq. (13) reproduces the "fluorescence particle counting" results of [12]. Under the same conditions on $\mathbf{r}_t$ and γ_k, but with an arbitrary radius of rotation, we find the recent results of [22] for the temporal autocorrelation in a laser scanning configuration. Finally, Enderlein has studied a closely related model, with $\mathbf{r}_t$ tracing a circular orbit for use in tracking control, by numerical simulation [15]. In that work, Monte Carlo simulation results including simple chemical kinetics are presented; we have studied these cases analytically for the tracking-FCS model presented here, and the results will be presented elsewhere.

As an example of the general tracking-FCS theory of Eq. (13), we calculate the fluctuations expected for our own experiment. Consider a particle with diffusion coefficient D symmetri-

#8420 - $15.00 USD Received 9 August 2005; revised 20 September 2005; accepted 21 September 2005

cally "trapped" along the x and y axes with rate γ_{xy} in a rotating radially symmetric Gaussian beam with transverse waist w_{xy}. for our experiment, γ_{xy} is exactly the feedback tracking bandwidth; *i.e.* it is the reciprocal of the (exponential) response time for a unit-step input to the tracking controller. The laser rotates at radius $w_{xy}\rho_0$ and angular frequency ω_0. In our experiment, microspheres are confined in the z direction by the boundaries of the sample volume, which we may take to be reflecting boundaries for the relevant case of low surface adhesion. Green's functions for free particle motion and corresponding fluorescence autocorrelation functions have been calculated as an infinite series for a Gaussian beam focused *symmetrically* between two reflecting planes [2]; the resulting series have been approximated efficiently in [27], but we are unaware of an extension of these results to reflecting planes in an *asymmetric* configuration. Instead of tackling this difficult analytical problem, we instead approximate the reflecting boundaries in a way that naturally fits the formalism developed here: we introduce a third Ornstein-Uhlenbeck particle trap in the z dimension with corresponding rate γ_z. This trap is *not* due to the closed-loop particle tracking in our case; it is simply a tractable approximation for two reflecting planes that are placed asymmetrically about the laser focus. For this case, we have $\mathbf{r}_t/w_x = (\rho_0\cos\omega_0 t, \rho_0\sin\omega_0 t, z_0)$. Defining

$$g(\tau) = \left(\frac{\zeta_{xy}^2}{1-\lambda_{\tau,xy}^2}\right)\left(\frac{\zeta_z}{\sqrt{1-\lambda_{\tau,z}^2}}\right)\exp\left[-4\rho_0^2\left(\frac{\zeta_{xy}}{1-\lambda_{\tau,xy}^2}\right)-4z_0^2\left(\frac{\zeta_z}{1+\lambda_{\tau,z}}\right)\right], \tag{14}$$

we find for the full fluorescence autocorrelation

$$G(\tau) = g(\tau)\exp\left[4\rho_0^2\left(\frac{\zeta_{xy}\lambda_{\tau,xy}}{1-\lambda_{\tau,xy}^2}\right)\cos\omega_0\tau\right] \tag{15}$$

The oscillations at ω_0 in Eq. (15) are an artifact of the laser rotation, and they occur at a much larger frequency than the servo response frequency γ_{xy} and the z relaxation time γ_z. We are more interested in the contribution of these latter relaxation rates, and their interaction with a particle's diffusion dynamics. In order to decouple these two effects, we may average the fluorescence correlation function over "coarse-grained" time bins, which are large compared to the rotation frequency but small compared to all other rates. Let us average $G(\tau)$ over bins of size $\tilde{T} \approx NT$, where $T = 2\pi/\omega_0$ is the rotation period. (There exists an integer N for which the approximation $\tilde{T} \approx NT$ is valid whenever $\tilde{T} \gg T$, and of course, the approximation is exact when $\tilde{T}$ is equal to an integer number of rotation periods.) Denoting the coarse-grained autocorrelation function by $\tilde{G}(\tau)$, we have

$$\tilde{G}(\tau) = \frac{1}{\tilde{T}}\int_{\tau-\tilde{T}/2}^{\tau+\tilde{T}/2} d\tau' G(\tau') d\tau' \approx \frac{g(\tau)}{\tilde{T}}\int_{\tau-\tilde{T}/2}^{\tau+\tilde{T}/2} d\tau' \exp\left[4\rho_0^2\left(\frac{\zeta_{xy}\lambda_{\tau,xy}}{1-\lambda_{\tau,xy}^2}\right)\cos\omega_0\tau'\right] d\tau' \tag{16}$$

where we have assumed that $g(\tau)$, $\lambda_{\tau,xy}$ and $\lambda_{\tau,z}$ are all approximately constant over the coarse grained time bin $\tilde{T}$. The remaining integral can be reduced to the form

$$\frac{1}{N\pi}\int_0^{N\pi} \exp[z\cos\theta]\, d\theta = I_0(z) \tag{17}$$

where I_0 is the modified Bessel function of order 0. After performing the integration in Eq. (16), we find

$$\tilde{G}(\tau) \approx g(\tau) I_0\left[4\rho_0^2\left(\frac{\zeta_{xy}\lambda_{\tau,xy}}{1-\lambda_{\tau,xy}^2}\right)\right] \tag{18}$$

#8420 - $15.00 USD Received 9 August 2005; revised 20 September 2005; accepted 21 September 2005

Equation (18) has the additional advantage that it represents an *average* of the shape of the laser over a rotation period. In our experiment, we expect that the laser is not particularly well-approximated by a rotating Gaussian excitation profile because we focus the laser into an aqueous solution using an oil-immersion objective. Even though the full expression for $G(\tau)$ is not particularly good in our case, the approximate expression matches the experimental data quite well. See Fig. 4. The fit parameters are consistent with the estimate of D from Fig. 3 for a transverse beam waist $w_{xy} = 1\ \mu$m. Furthermore, the tracking bandwidth of 134 Hz matches well with the electronic design parameters and the 200 Hz designed bandwidth in [18]. The fit parameters indicate a confinement in the z direction of $\sqrt{D/\gamma_z} = 1.4\mu$m, which is also consistent with independent estimates. In summary, the tracking-FCS theory based on Ornstein-Uhlenbeck particle statistics provides a very accurate model of the fluorescence fluctuations in closed-loop particle tracking. Furthermore, we have shown that fits to this theory may provide accurate measurements of feedback control parameters and intrinsic particle diffusion properties.

Finally, note that the experimenter may choose the laser rotation frequency ω_0 to be much faster than whatever dynamics he or she wishes to measure. By increasing the number of periods over which the lock-in signal is integrated, the choice of ω_0 will not affect the signal-to-noise ratio of the position estimation. Thus, the utility of the coarse-grained approximation is not restricted to the timescales presented here, nor does it in principle reduce the time-resolution of the tracking-FCS method. To resolve faster oscillations in the fluorescence autocorrelation curve, the experimenter simply needs to choose a sufficiently large ω_0, then average over these oscillation in the data analysis. On the other hand, fluorescence fluctuations on timescales *faster* than the laser rotation frequency are also decoupled in the autocorrelation curve. It therefore simply remains for the experimenter to choose a laser rotation frequency outside of the dynamical timescale of interest, which may be done in principle with no degradation of tracking performance.

4. Conclusions

In this paper, we have discussed the implementation and interpretation of diffusion estimates and fluorescence autocorrelation measurements for the case that an *individual* particle is actively tracked by real-time feedback control methods. The results of this paper are twofold: first, we presented a simplified method of particle tracking using fluorescence modulation/demodulation techniques. Second, we presented a full theory of fluorescence fluctuations in the case that a particle's motion is not so slow that the controller may be considered "perfect." The key concept that underlies the tracking-FCS theory is the separation of *controlled* motion, represented by Ornstein-Uhlenbeck trapping statistics, uncontrolled but deterministic motion of the laser centroid, and uncontrolled Brownian motion. The tracking-FCS theory naturally unites closed-loop control parameters, such as the feedback controller's step response time γ_{xy}, with dynamical parameters such as the particle's diffusion coefficient D. Furthermore, the coarse-grained approximation suppresses the large amplitude (deterministic) oscillations in a measured fluorescence autocorrelation curve, thus reducing the apparent experimental artifacts in measured results. The theory presented here should be immediately applicable to three-dimensional tracking of the type in [20]; furthermore, the theory should apply equally well to fluorescence fluctuations in the case that a particle is trapped by external forces as well. We hope that the tracking-FCS methods presented here will become useful in the same way that FCS allows the measurement of stochastic dynamical processes, with a simple underlying theoretical basis.

Eventually, we expect these techniques to be useful for the measurement of stochastic dynamics in single molecules in a biologically compatible environment, with single shot reso-

#8420 - $15.00 USD Received 9 August 2005; revised 20 September 2005; accepted 21 September 2005

lution over many orders of magnitude in time. However, it is natural to ask whether a single dye-labelled biomolecule is bright enough to enable closed-loop tracking of the type described here. In a separate theoretical analysis [28], we have studied the fluorescence and bandwidth regimes where a particle can be tracked by the methods described here (including a three-dimensional generalization) and find that tracking single molecules with typical diffusion coefficients of order $1\mu\mathrm{m}^2/\mathrm{s}$ and detected photon count rates as low as $10^4\mathrm{s}^{-1}$ should be feasible with the present techniques. A complementary question arises in the single-fluorophore case: since typical fluorophores may only emit a total of $\sim 10^6$ photons before photobleaching, the absolute length of time over which a single fluorophore may be tracked is limited. However, beautiful recent experiments have revealed folding transitions in single ribozymes [29, 30] and proteins [31] using surface tethering and vesicle encapsulation techniques for increasing observation times. In these experiments, fluorescence signals sufficiently above background rates are typically collected over a few (1-10) seconds from each individual observed molecule. If we consider an optimistic confocal detection efficiency of $\sim 10\%$, and a fluorescence count rate of $2.5\times 10^4\mathrm{s}^{-1}$, we may expect to use the techniques described here to track (and observe) a single dye-labelled biomolecule for a time ~ 4s, which is sufficient for revealing these (and presumably other) interesting conformational transitions. The tracking-FCS methods presented here may then be useful for further resolving faster conformational and kinetic dynamics, such as those accessible by traditional FCS, on *individual* molecules with no ensemble averaging.

Acknowledgments

We thank K. McHale for discussions of statistical estimation and C. Lee for experimental assistance. This work was supported by the Institute for Collaborative Biotechnologies through grant DAAD19-03-D-0004 from the U.S. Army Research Office and by the NSF through grants DBI-0242705 and EIA-0323542.

A. Derivation of Equation (9)

In this Appendix, we will present a brief derivation of Eq. (9) in a more general setting. Let X_t be a real-valued stochastic process, and let $\Phi_t(x)$ be some deterministic (sure) function of x, indexed by the time t. Here, we do not make any restriction on the form of Φ_t or X_t, except that X_t is at least ergodic and homogenous (that is, stationary in the long-time limit [25]). Homogeneity ensures that the steady-state distributions

$$P_0(x) \equiv \lim_{t\to\infty} P(X_t = x) \tag{19}$$

$$P_\tau(x_2|x_1) \equiv \lim_{t\to\infty} P(X_{t+\tau} = x_2 | X_t = x_1) \tag{20}$$

are well-defined. Neglecting photon arrival time statistics, we may consider $\Phi_t(x)$ to be the rate of photon arrivals from a particle at position x at time t. The stochastic, time-dependent photon arrival rate σ_t is then a sure function of the stochastic particle position X_t: $\sigma_t = \Phi_t(X_t)$. Its autocorrelation function is given by

$$G(\tau) = \langle \sigma_t \sigma_{t+\tau} \rangle_t = \langle \Phi_t(X_t)\Phi_{t+\tau}(X_{t+\tau})\rangle_t \,. \tag{21}$$

Rewriting the right-hand side of Eq. (21) in terms of $\tilde{\Phi}_t(q)$, the Fourier transform of $\Phi_t(x)$, we have

$$\begin{aligned} G(\tau) &= \left\langle \iint \frac{dq_1}{2\pi}\frac{dq_2}{2\pi} e^{-iq_1X_t - iq_2X_{t+\tau}} \tilde{\Phi}_t(q_1)\tilde{\Phi}_{t+\tau}(q_2) \right\rangle_t \\ &= \iint \frac{dq_1}{2\pi}\frac{dq_2}{2\pi} \left\langle e^{-iq_1X_t - iq_2X_{t+\tau}} \right\rangle_t \left\langle \tilde{\Phi}_t(q_1)\tilde{\Phi}_{t+\tau}(q_2)\right\rangle_t \end{aligned} \tag{22}$$

#8420 - $15.00 USD Received 9 August 2005; revised 20 September 2005; accepted 21 September 2005

where the factorization of the time-averages in the second line follows from the fact that the functions Φ_t are *sure*, and are therefore uncorrelated with functions of X_t. We now invoke the assumption that X_t is an ergodic process, so that we may equate the left-most bracketed term in Eq. (22) to an average over *realizations* of X_t. We then find

$$\left\langle e^{-iq_1X_t - iq_2X_{t+\tau}} \right\rangle_t = \iint dx_1 dx_2 e^{-iq_1x_1} e^{-iq_2x_2} P_0(x_1) P_\tau(x_2|x_1). \tag{23}$$

This is just the characteristic function for the joint process $(X_t, X_{t+\tau})$, which exists for all suitably bounded real-valued processes X_t [26]. Inserting Eq. (23) into Eq. (22), we note that $\tilde{\Phi}_t$ and $\tilde{\Phi}_{t+\tau}$ are the only remaining functions of t. We may therefore pull the time averaging brackets outside the integrals and perform the integrals over q_1 and q_2 to find

$$G(\tau) = \left\langle \iint dx_1 dx_2 P_0(x_1) P_\tau(x_2|x_1) \Phi_t(x_1) \Phi_{t+\tau}(x_2) \right\rangle_t . \tag{24}$$

Taking $\Phi_t(x_1) = \Phi_x(x_1 - w_x\chi_t)$, and substituting Eqs. (7) and (8) into Eq. (24), we have the desired result for Eq. (9).

#8420 - $15.00 USD Received 9 August 2005; revised 20 September 2005; accepted 21 September 2005